scientific reports

Check for updates

OPEN

TNF-α induces mitochondrial dysfunction to drive NLRP3/Caspase-1/GSDMD-mediated pyroptosis in MCF-7 cells

Kexin Gao[1], Yancui Liu[1], Cheng Sun[1], Ying Wang[1], Hongrong Bao[1], Guoyang Liu[2], Jinrui Ou[3] & Ping Sun[1]✉

Pyroptosis is a gasdermin-mediated pro-inflammatory form of programmed cell death (PCD). Tumor necrosis factor-α (TNF-α) is an inflammatory cytokine, and some studies have shown that TNF-α can cause pyroptosis of cells and exert anti-tumor effects. However, whether TNF-α exerts anti-tumor effects on breast cancer cells by inducing pyroptosis has not been reported. In this study, to explore the impact of TNF-α on pyroptosis in breast cancer cells, we treated MCF-7 cells with TNF-α and found that TNF-α induced cell death. Moreover, we observed that the dead cells were swollen with obvious balloon-like bubbles, which was a typical sign of pyroptosis. Further studies have found that the anti-tumor effect of TNF-α on breast cancer cells in vitro was achieved through the canonical pyroptosis pathway. In addition, TNF-α-induced pyroptosis in MCF-7 cells was associated with mitochondrial dysfunction, in which mitochondrial membrane potential was decreased and mitochondrial ROS production was increased. After inhibiting ROS production, the activation effect of TNF-α on NLRP3/Caspase-1/GSDMD pathway was weakened, and the inhibitory effect of TNF-α on the growth of MCF-7 cells in vitro was also decreased, further confirming the involvement of ROS in TNF-α-induced pyroptosis. Overall, our study revealed a new mechanism by which TNF-α exerts an anti-tumor effect by inducing pyroptosis in MCF-7 cells through the ROS/NLRP3/Caspase-1/GSDMD pathway, which may provide new therapeutic ideas for the treatment of breast cancer.

Keywords TNF-α, Pyroptosis, ROS, Breast cancer

Breast cancer (BC) is a common malignant tumor, ranking first in both morbidity and mortality among female malignancies and posing a severe threat to women's lives and health[1]. Over the years, researchers have found that cell death is closely related to tumorigenesis and progression of BC. Inducing programmed cell death (PCD) has become an important means of BC treatment[2–7]. Apoptosis, a major PCD, has long been considered an important mechanism for preventing the emergence of BC and has been widely studied[8]. However, since one of the characteristics of tumors is to escape apoptosis, finding other non-apoptotic programmed cell death modalities is essential for BC treatment.

Tumor necrosis factor (TNF) was first identified in 1975 from activated macrophages, natural killer cells (NK cells), and T lymphocytes[9]. In 1985, Shalaby named the TNF produced by macrophages TNF-α. As a pleiotropic cytokine, TNF-α plays a vital role in cell survival and death[10]. Studies have shown that TNF-α has a broad spectrum of cytotoxic effects on various cancer cells, such as colorectal cancer, lung cancer, and sarcoma[11]. TNF-α has shown a crucial anti-tumor activity in breast cancer cells as well. It is found that high levels of TNF-α are related to a reduced risk of breast cancer progression. Furthermore, TNF-α can inhibit the growth of ER-positive breast cancer cells by influencing cell cycle progression[12]. Many studies have also confirmed the anti-tumor effect of TNF-α by inducing apoptosis in breast cancer cells. For example, it has been found that TNF-α exerts cytotoxic effects and induces apoptosis in MCF-7 cells. In addition, claudin-1 exerts an anti-apoptotic effect on TNF-α-induced apoptosis in MCF-7 cells[13]. Gelsolin-mediated ROS production also has important

[1]Department of Anatomy, Mudanjiang Medical University, Mudanjiang City 157000, Heilongjiang, China. [2]Department of Nuclear Medicine, Hongqi Hospital affiliated to Mudanjiang Medical University, Mudanjiang City 157000, Heilongjiang, China. [3]Department of Nuclear Magnetic, the Second People's Hospital of Mudanjiang City, Mudanjiang City 157000, Heilongjiang, China. ✉email: 794988268@qq.com

implications for TNF-α-induced apoptosis in MCF-7 cells[14]. Nevertheless, whether TNF-α can exert an anti-tumor effect on MCF-7 cells through other non-apoptotic PCD pathways has not been reported.

Like apoptosis, pyroptosis has recently been found to play an essential role in the development of tumorigenesis. Pyroptosis is a new form of pro-inflammatory PCD characterized by cell swelling, balloon-like bubbles forming on cell membranes, cell rupture, and release of cell contents[15]. The canonical pathway dependent on Caspase-1 activation was the first identified pyroptosis pathway, and studies have shown that the activation of NLRP3 inflammasome plays a vital role in this process[16–18]. Stimulated by danger signals like pathogens, intracellular pattern recognition receptors recognize these signals and bind to Caspase-1 precursors through the adaptor protein apoptosis-associated speck-like protein containing a CARD (ASC) to form the NLRP3 inflammasome. Inflammasomes can activate Caspase-1 to cleave GSDMD further, and the GSDMD-N terminus can induce cell membrane perforation, thereby promoting pyroptosis[19,20]. In the non-canonical pathway, Caspase-4,5,11 are activated under the stimulation of LPS and other signals, and GSDMD is cleaved to produce GSDMD-N to induce pyroptosis. In addition, studies have found that specific stimuli lead to the activation of Caspase-3, and the activated Caspase-3 cleaves GSDME to produce an N-terminal fragment (GSDME-N), which is also involved in the pore formation and leads to cell pyroptosis[21,22]. Recently, emerging studies have demonstrated that pyroptosis plays a crucial role in tumor progression, and inducing pyroptosis has also become one of the critical hot spots in BC immunotherapy[23]. TNF-α has been found to activate Caspase-3 to cleave GSDME and transform apoptosis into pyroptosis to inhibit tumor growth[24]. However, the potential mechanisms by which TNF-α exerts its anti-cancer effect via regulation of pyroptosis in BC remains unclear.

In this study, we first detected the effect of TNF-α on pyroptosis and NLRP3/Caspase-1/GSDMD pathway in MCF-7 cells. Second, we investigated whether mitochondrial dysfunction participated in TNF-α-mediated pyroptosis. Finally, we assessed the role of ROS caused by mitochondrial dysfunction in TNF-α-induced pyroptosis. We found that TNF-α induced NLRP3/Caspase-1/GSDMD-mediated pyroptosis by regulating mitochondrial dysfunction to increase mitochondrial ROS production, thereby inhibiting the proliferation of MCF-7 cells.

Results

TNF-α inhibited cell proliferation and induced pyroptosis in MCF-7 cells

We first treated MCF-7 cells with different concentrations of TNF-α for 48 h to observe the effect of TNF-α on the proliferative ability of breast cancer cells. The results showed that the viability of MCF-7 cells treated with TNF-α decreased in a dose-dependent manner (Fig. 1A). The colony formation assay further verified the inhibitory effect of TNF-α on the growth of MCF-7 cells (Fig. 1B, C). Subsequently, we explored whether TNF-α-induced cell death was associated with pyroptosis. We found that compared with the control group, cells in the TNF-α treatment group were swollen, and large bubbles were blown out of the cell membrane, which was a distinct pyroptosis morphology (Fig. 1D). Due to membrane rupture, PI can stain pyroptosis cells. Figure 1E and F showed that PI-positive cells gradually increased after TNF-α treatment. Pyroptosis cell membrane rupture leads to the release of cell contents. Thus, we measured the amount of LDH in the supernatant of MCF-7 cells in different groups. We found that TNF-α treatment significantly increased LDH release in a dose-dependent manner, suggesting that TNF-α disrupted the integrity of MCF-7 cells (Fig. 1G). Besides, we examined the release of cellular inflammatory cytokines in MCF-7 cells after TNF-α treatment. We found that IL-1β and IL-18 expression were significantly increased in the supernatant of the cells after using TNF-α (Fig. 1H, I). The above experiments showed that TNF-α inhibited cell growth and induced pyroptosis in MCF-7 cells.

TNF-α induced pyroptosis in MCF-7 cells through NLRP3/Caspase-1/ GSDMD pathway

To investigate the underlying mechanism of TNF-α-induced pyroptosis in MCF-7 cells, we stimulated MCF-7 cells with TNF-α at concentrations of 50 or 100 ng/ml for 48 h. Then, we detected the expression levels of pyroptosis-related proteins by western blot (Fig. 2A). The results showed that the expression level of NLRP3 protein was increased after TNF-α treatment compared with the control group, suggesting that NLRP3 inflammasome may be activated (Fig. 2B). Meanwhile, the expression of activated Caspase-1 and GSDMD-N with perforation activity were also up-regulated after TNF-α treatment, suggesting that the classical pyroptosis pathway was involved in TNF-α-induced MCF-7 cell death (Fig. 2C, D). Immunofluorescence staining further confirmed the result (Fig. 2E, F). These results implied that TNF-α induced NLRP3/Caspase-1/GSDMD pathway-mediated pyroptosis in MCF-7 cells. Next, we applied the NLRP3 inhibitor MCC950 to inhibit this pathway and observe the effect on cell viability. A significant reduction in MCF-7 cell deaths after inhibition of NLRP3 was observed under the microscope (Fig. 2G). The CCK-8 assay further detected the inhibition effect of NLRP3 on the viability of MCF-7 cells and found that the application of MCC950 partially reversed the inhibitory effect of TNF-α on the growth of MCF-7 cells (Fig. 2H). These results suggested that TNF-α-induced MCF-7 mortality was partially achieved due to NLRP3/Caspase-1/GSDMD pathway-mediated pyroptosis.

TNF-α-induced mitochondrial dysfunction promoted pyroptosis in MCF-7 cells

We further explored the underlying mechanism by which TNF-α induced pyroptosis in MCF-7 cells. Since multiple studies have shown that mitochondria are essential in regulating pyroptosis, we first explored whether mitochondria are involved in TNF-α-induced pyroptosis in MCF-7 cells. By performing immunofluorescence assays on GSDMD and mitochondrial staining, we found that GSDMD and mitochondrial co-localization were more pronounced after TNF-α treatment, suggesting that mitochondria may be involved in TNF-α-induced pyroptosis in MCF-7 cells (Fig. 3A, B).

Next, we evaluated the effect of TNF-α treatment on the mitochondrial function of MCF-7 cells. We observed the changes in the mitochondrial membrane potential of MCF-7 cells after JC-1 staining by fluorescence microscopy. The results showed that TNF-α treatment reduced the ratio of JC-1 aggregates (red) to monomers

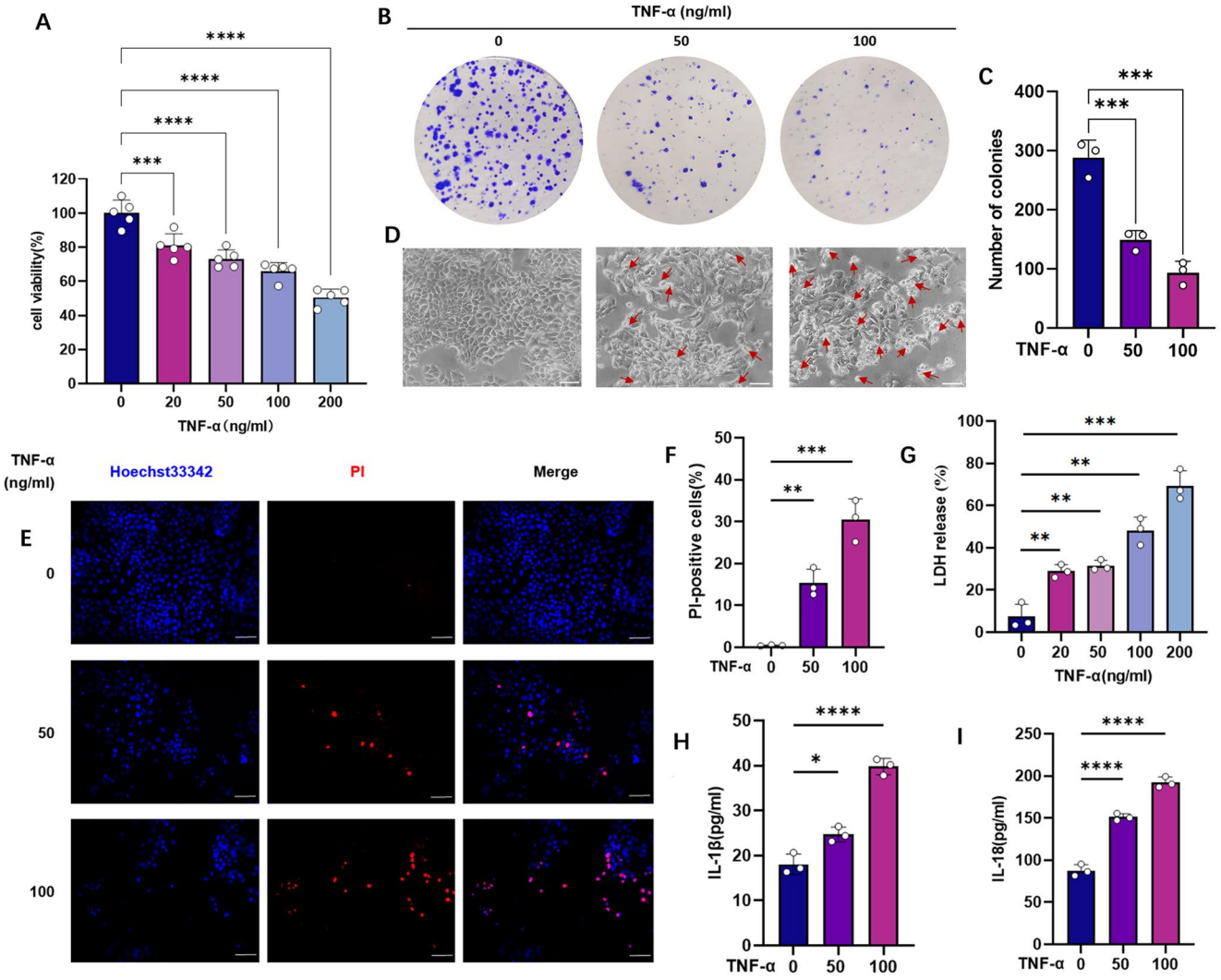

Figure 1. TNF-α inhibited cell growth and induced cell pyroptosis in MCF-7 cells. (**A**) Cell viability of MCF-7 cells after treatment with various concentrations of TNF-α (0, 20, 50, 100,200 ng/ml) for 48 h was detected by CCK-8 assay. (**B**) The inhibitory effect of TNF-α on colony formation of MCF-7 cells. (**C**) Quantitative analysis of colony formation assay.**(D)**Representative microscopic images of MCF-7 cells treated with TNF-α. Red arrows indicate pyroptotic cells. (**E**) Fluorescence microscopy images of MCF-7 cells stained with Hoechst 33342(Blue, staining nucleus) and PI (Red, staining dying cells) after TNF-α treatment. (**F**) Statistical analysis of the percentage of PI-positive cells. (**G**) LDH release in the supernatant of each group after TNF-α treatment. (**H**, **I**) The contents of IL-18 and IL-1β in the supernatant of MCF-7 cells after TNF-α treatment. $^{*}P < 0.05$;$^{**}P < 0.01$;$^{***}P < 0.001$; $^{****}P < 0.0001$. Scale bars, 50 μm.

(green) compared with the control group, indicating a decrease in mitochondrial membrane potential and depolarization of mitochondria (Fig. 3C, D). Since mitochondrial depolarization is closely associated with ROS production, we detected intracellular ROS expression after TNF-α treatment. DCFH-DA dye was used to stain ROS, and it can be seen that TNF-α treatment significantly increased the production of cellular ROS (Fig. 3E, F). Mitochondria are the primary source of ROS, and we further stained mitochondria and ROS to observe whether TNF-α-induced ROS production was derived from mitochondria and the results showed that TNF-α treatment increased the fluorescence intensity of selective mitochondrial ROS in MCF-7 cells, indicating that TNF-α induced mitochondrial ROS production (Fig. 3G, H). These results suggested that TNF-α-induced pyroptosis was associated with mitochondrial dysfunction and ROS accumulation.

TNF-α induced pyroptosis was reversed by NAC treatment

To verify the role of ROS in TNF-α-induced pyroptosis in MCF-7 cells, we first pretreated the cells with ROS scavenger (NAC) for 2 h and then applied TNF-α. It was seen that NAC significantly suppressed the increase of ROS in MCF-7 cells induced by TNF-α (Fig. 4A, B). Besides, NAC treatment significantly reversed the TNF-α-induced decrease in MCF-7 cell viability (Fig. 4C). Clone formation experiments showed that the number of MCF-7 cell clones formed significantly increased after ROS inhibition compared with the TNF-α treatment

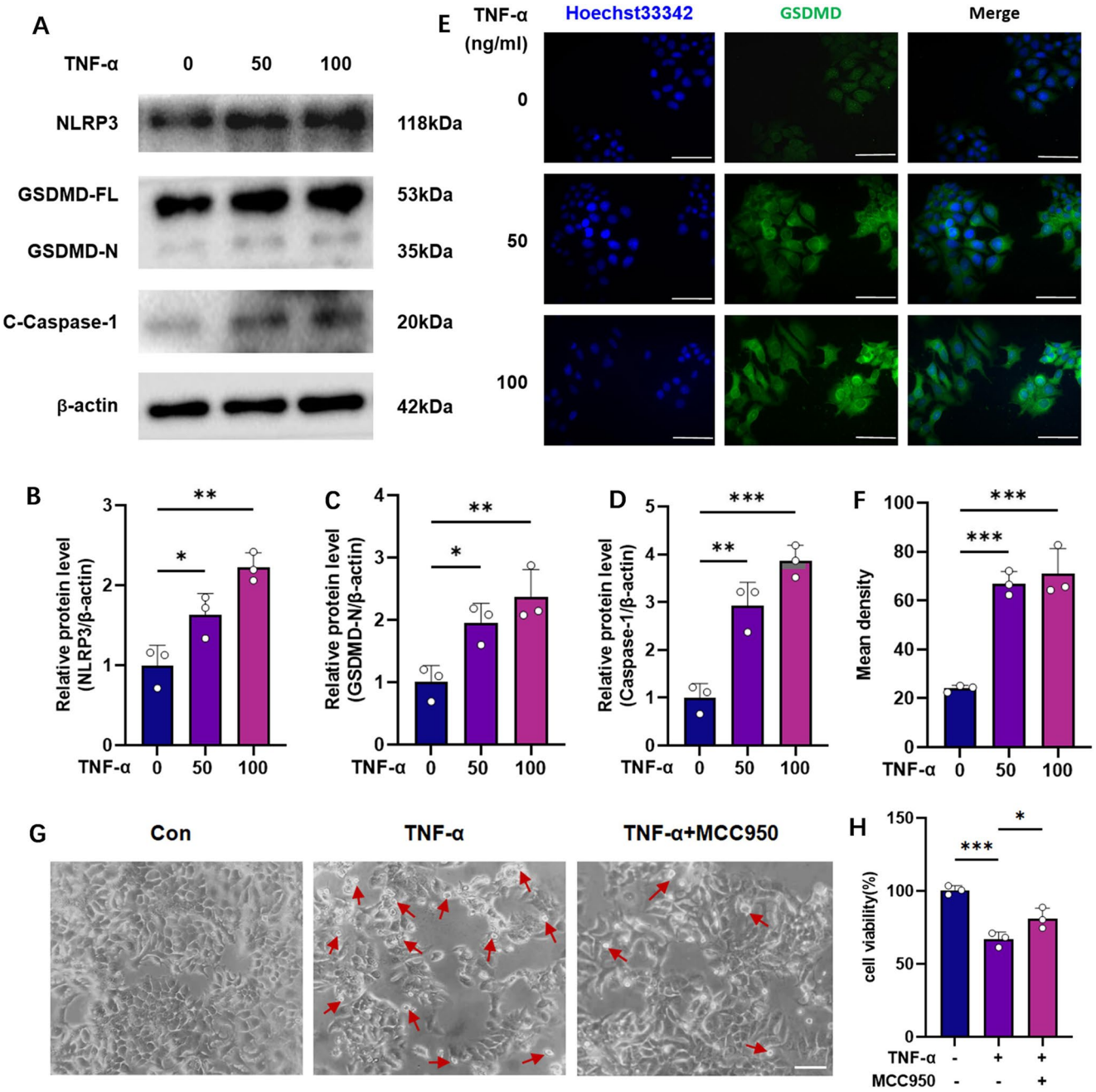

Figure 2. TNF-α induced pyroptosis in MCF-7 cells through NLRP3/Caspase-1/ GSDMD pathway. (**A**) Western blot analysis of pyroptosis-related proteins in MCF-7 cells with indicated concentrations of TNF-α for 48 h. β-actin was included as a loading control. (**B-D**) Quantitative results of NLRP3, Cleaved-Caspase-1, and GSDMD-N in MCF-7 cells. (**E**) Representative immunofluorescence microscopy images of GSDMD in MCF-7 cells. (**F**) Quantitative results of relative fluorescence intensity of GSDMD from random regions of the images. (**G**) Representative microscopic images of MCF-7 cells in different groups. (**H**) CCK-8 detected the inhibition effect of MCC950 on cell viability. *$P<0.05$;**$P<0.01$; *** $P<0.001$.Scale bars, 50 μm.

group (Fig. 4D, E). We also found that NAC treatment inhibited TNF-α-induced pyroptosis and decreased the number of cells and pyroptosis morphology blown out of the plasma membrane (Fig. 4F). Meanwhile, the number of PI-positive cells and the release of LDH were reduced as well (Fig. 4G-I). The release of IL-1β and IL-18 were decreased in the cell supernatant after NAC treatment (Fig. 4J, K). The above results indicated that TNF-α-induced pyroptosis was reversed by NAC treatment.

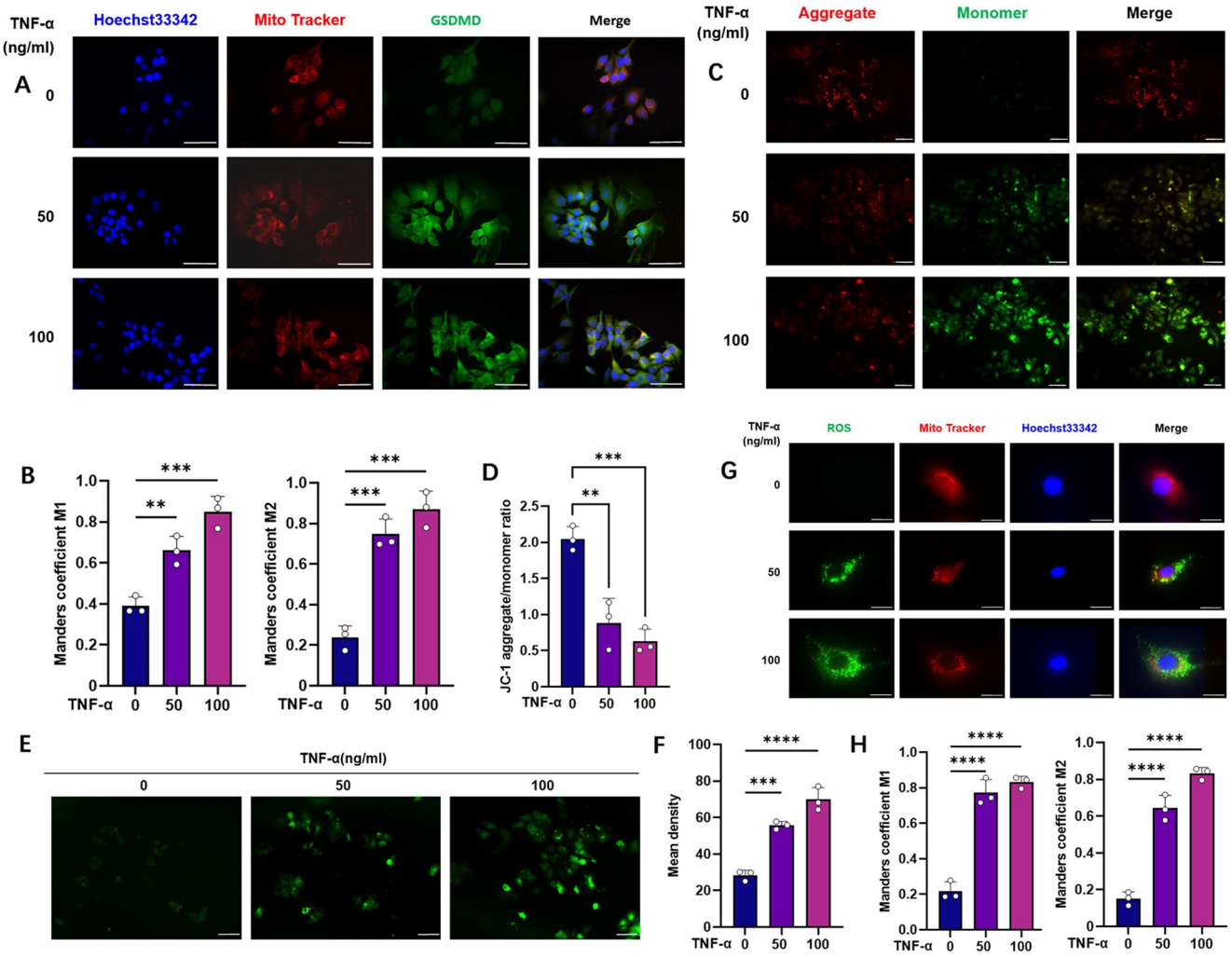

Figure 3. TNF-α-induced mitochondrial dysfunction promoted pyroptosis in MCF-7 cells. MCF-7 cells were treated with indicated concentrations of TNF-α for 48 h. (**A**) Immunostaining of GSDMD and the mitochondria in MCF-7 cells. (**B**) Co-localization analysis plot of GSDMD with mitochondria. (**C**) Fluorescence microscopy images of Mitochondrial membrane potential (ΔΨm) in MCF-7 cells measured by a JC-1 assay kit. (**D**) Statistical graph of the ratios of JC-1 aggregates /monomer. (**E**) Fluorescence microscopy images of ROS measured by a DCFH-DA probe. (**F**) Quantitative results of relative fluorescence intensity of ROS from random regions of the images. (**G**) Fluorescence microscopy images of the subcellular location of ROS in MCF-7 cells labeled with the probe DCFH-DA and MitoTracker Red CMXRos. (**H**) Co-localization analysis plot of ROS and mitochondria. $^{**}P < 0.01$; $^{***}P < 0.001$; $^{****}P < 0.0001$. Scale bars, 50–25 μm.

Reduction of ROS generation inhibited NLRP3/Caspase-1/GSDMD-mediated pyroptosis induced by TNF-α

Next, we explored the inhibitory effect of ROS on the TNF-α-induced classical pyroptosis. We found that NAC pretreatment significantly reduced the expression of pyroptosis-related proteins, including NLRP3, C-Caspase-1 and GSDMD-N in MCF-7 cells (Fig. 5A-D). Immunofluorescence analysis further verified the inhibitory effect of NAC on GSDMD (Fig. 5E, F). These results demonstrated that ROS played an essential role in TNF-α-induced pyroptosis.

Discussion

Cell death has a significant influence on internal environmental homeostasis and disease development[25]. The tumorigenesis is marked by a successful evasion of the regulation of cell death to achieve unlimited replication. As the most common malignant tumor in women, the incidence of breast cancer has been increasing since the 1970s and has now become one of the central diseases of female death around the world[26]. Increasing evidence has demonstrated the importance of cytokines exerting their biological function against breast cancer[27]. As a cytokine with various biological functions, TNF-α has potent anti-tumor activity, which can kill some tumor cells in vivo and in vitro and inhibit tumor cell proliferation[11,28]. Recombinant TNF-α has been successfully prepared and gradually applied to treat tumors[29,30]. Our experiments confirmed that TNF-α significantly

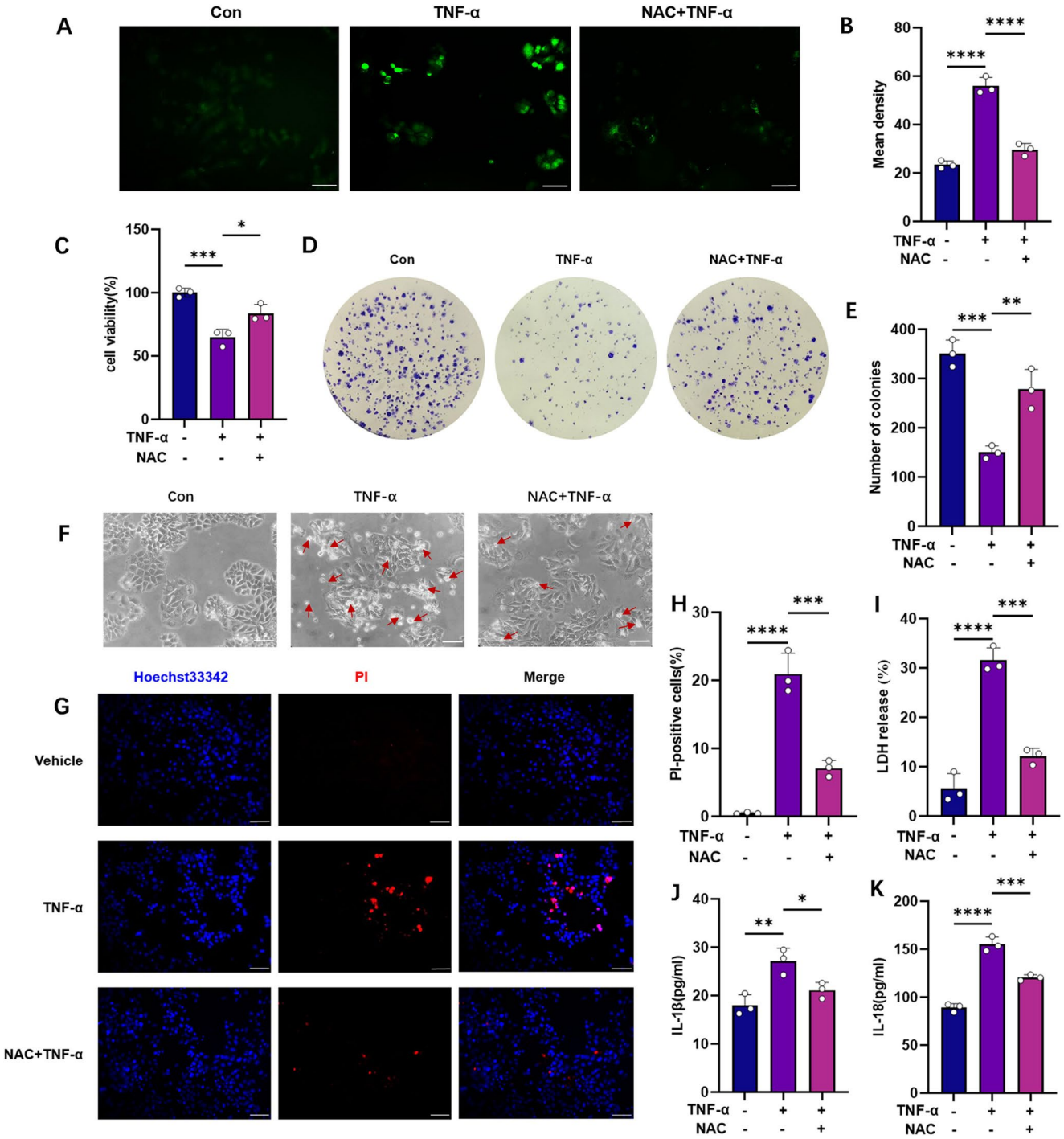

Figure 4. TNF-α induced pyroptosis was reversed by NAC treatment. MCF-7 cells were pretreated with or without 5 mM NAC for 2 h and then treated with indicated concentrations of TNF-α (50 ng/ml) for another 48 h. (**A**) Fluorescence microscopy images of ROS measured by a DCFH-DA probe. (**B**) Quantitative results of relative fluorescence intensity of ROS from random regions of the images. (**C**) CCK-8 detected the inhibition effect of NAC on cell viability. (**D**) Colony formation of MCF-7 cells in each group. (**E**) Quantitative analysis of colony formation assay. (**F**) Representative microscopic images of MCF-7 cells in different groups. Red arrows indicate pyroptotic cells. (**G**) Fluorescence microscopy images of MCF-7 cells stained with Hoechst 33342 and PI. (**H**) Statistical analysis of the percentage of PI-positive cells. (**I**) LDH release in the supernatant of MCF-7 cells in different groups. (**J**, **K**) Effect of NAC treatment on the contents of IL-18 and IL-1β in the supernatant of MCF-7 cells. * $P<0.05$;** $P<0.01$; *** $P<0.001$; **** $P<0.0001$. Scale bars,50 μm.

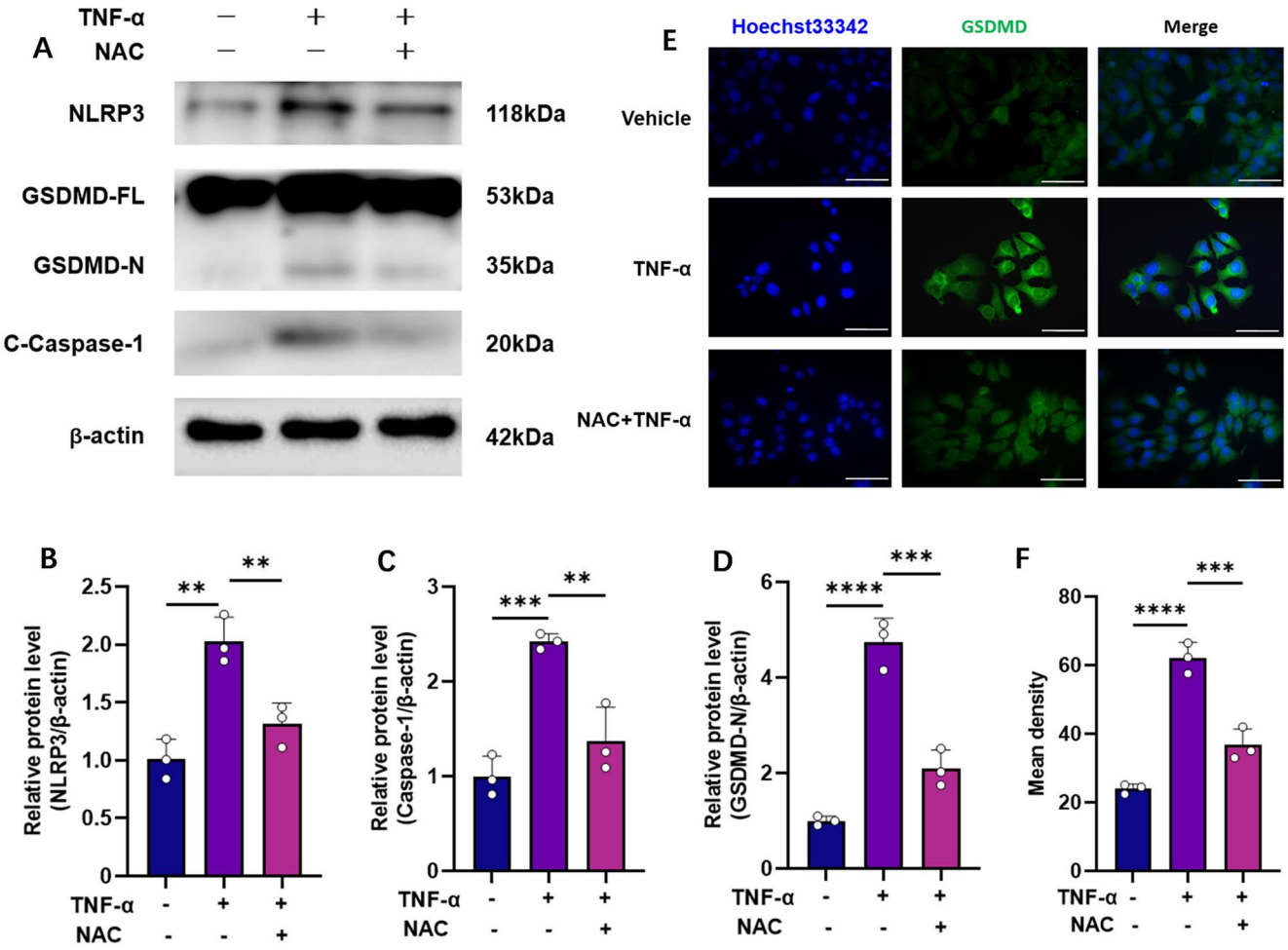

Figure 5. Reduction of ROS generation inhibited NLRP3/Caspase-1/GSDMD-mediated pyroptosis induced by TNF-α. MCF-7 cells were pretreated with or without 5 mM NAC for 2 h and then treated with indicated concentrations of TNF-α (50 ng/ml) for another 48 h. (**A**) Western blot analysis of NLRP3, Cleaved-Caspase-1, and GSDMD-N expression in MCF-7 cells. β-actin was included as a loading control. (**B**-**D**) Quantitative results of NLRP3, Cleaved-Caspase1, and GSDMD-N in different groups. (**E**) Representative immunofluorescence microscopy images of GSDMD in MCF-7 cells. (**F**) Quantitative results of relative fluorescence intensity of GSDMD from random regions of the images. $^{**}P < 0.01$; $^{***}P < 0.001$; $^{****}P < 0.0001$. Scale bars,50 μm.

inhibited the proliferation of MCF-7 cells by CCK-8 and colony formation assay. Many studies have shown that TNF-α can induce apoptosis and arrest the cell cycle in various cancer cells, thereby inhibiting the growth of cancer cells[13,31,32]. Further studies are needed to explore whether TNF-α exerts an anti-tumor effect on breast cancer cells via other non-apoptotic PCD pathways.

Pyroptosis is a PCD that can cause severe inflammatory responses, and TNF-α was initially found to induce pyroptosis in inflammatory diseases. The inflammatory signaling pathway involved in TNF-α plays a crucial role in pyroptosis in acute kidney injury (AKI) and acute liver failure (ALF)[33]. In addition, inhibition of TNF-α-induced Caspase-3/GSDME-mediated cell pyroptosis can alleviate rheumatoid arthritis[34]. Another study found that idiopathic pulmonary fibrosis (IPF) is mainly due to the production of pro-inflammatory factor TNF-α then activates the NF-κB signaling pathway to induce inflammasome including NLRP3 and cause pyroptosis through a series of cascade reactions[35]. With further research, TNF-α-induced pyroptosis has been proven to be associated with the development of various cancers. TNF-α and gemcitabine induce Caspase-3/GSDME-mediated pyroptosis in pancreatic cancer cells and release numerous inflammatory factors. Furthermore, TNF-α treatment can activate Caspase-8 to cleave GSDMC to produce GSDMC-N to induce pyroptosis in cancer cells[36]. The combination of TNF-α and cycloheximide (CHX) can activate BAK/BAX and induce Caspase-3-GSDME-mediated pyroptosis in colorectal cancer cells with high GSDME expression[37]. Inducing pyroptosis in breast cancer cells can inhibit the development of cancer. However, whether TNF-α exerts an anti-tumor effect on breast cancer by inducing pyroptosis has not been studied. Through experimental studies, we found that TNF-α-treated MCF-7 cells were swollen and ruptured, bubbles were blown out of the cell membrane, and cell contents were released, suggesting that cells may undergo pyroptosis. Studies have shown that the activation of NLPP3 can lead to pyroptosis and the release of pro-inflammatory factors, and the activation of inflammasomes in

tumors plays a vital role in anti-tumor immunity. In this study, we found that TNF-α treatment promoted the formation of NLRP3 inflammasome, which further activated Caspase-1 to become active C-Caspase-1 and then cleaved GSDMD to produce GSDMD-N fragments with perforated activity and eventually caused pyroptosis in MCF-7 cells. Our present findings raise the question of how TNF-α induces pyroptosis through the canonical pathway in MCF-7 cells.

Mitochondrial dysfunction can lead to the production of cellular ROS, and many studies have confirmed that ROS plays an essential role in many types of cell death, such as apoptosis, necrosis, and pyroptosis[38–43]. Mitochondrial ROS can promote NLRP3 inflammasome-dependent pyroptosis. Xie et al. find that Simvastatin inhibits colon cancer growth through the ROS/Caspase-1/GSDMD-mediated pyroptosis pathway[44]. In addition, hydrogen induces pyroptosis in endometrial cancer cells through the ROS/NLRP3/Caspase-1/GSDMD pathway[45]. A recent study found that mitochondrial ROS is involved in tetraarsenic hexoxide-induced Caspase-3/GSDME-mediated pyroptosis in triple-negative breast cancer cells, thereby exerting anti-tumor effects[46]. Based on the above studies, we speculate that ROS may be involved in TNF-α-induced pyroptosis in MCF-7 cells. Notably, we found that TNF-α induced mitochondrial dysfunction, and the production of mitochondrial ROS was increased after TNF-α treatment. The addition of antioxidants (NAC) significantly reduced the elevated ROS levels induced by TNF-α. Moreover, with the decrease of ROS, the TNF-α-induced pyroptosis of MCF-7 cells was also reduced, and the inhibitory effect on MCF-7 cell growth in vitro was also weakened. The specific mechanism of TNF-α-induced pyroptosis in breast cancer cells is shown in Fig. 6.

In summary, our study confirmed that TNF-α treatment led to mitochondrial dysfunction, which induced pyroptosis in MCF-7 cells through ROS / NLRP3 / Caspase-1 / GSDMD pathway. The study enriches the research on the anti-tumor effects of TNF-α and provides a meaningful reference for breast cancer-related experiments and treatments.

Materials and methods

Chemicals and reagents

Recombinant Human TNF-α was purchased from PeproTech (New Jersey, USA). MCC950 was bought from Aladdin (Shanghai, China). Fetal Bovine Serum (FBS), Dimethyl Sulfoxide (DMSO), and Dulbecco's Modified Eagle Medium (DMEM) were obtained from Gibco (Grand Island, NY, USA). RIPA Lysis Buffer, Loading Buffer, Protease Inhibitors, Hoechst 33342 and Propidium Iodide (PI), LDH Cytotoxicity Assay Kit, ROS Assay Kit, Mitochondrial membrane potential assay kit (JC-1), Mito-Tracker Red CMXRos and N-acetyl-L-cysteine (NAC) were bought from Beyotime Biotechnology (Shanghai, China). Human IL-18 Elisa Kit and Human IL-1β Elisa Kit were purchased from Jingkang Bioengineering Company (Shanghai, China). PVDF membranes were supplied from Roche (Basel, Switzerland). Tween and Trypsin Penicillin-Streptomycin were purchased from Biosharp (Anhui, China). PageRuler Prestained Protein Ladder was bought from Thermo Fisher Scientific (Massachusetts, USA). ECL reagent was purchased from GE Healthcare (Little Chalfont, UK). Antibodies specific to NLRP3, C-Caspase-1, GSDMD, and β-actin were supplied from Affinity (Cincinnati, OH, USA). The secondary antibodies, including Horseradish Peroxidase (HRP)-conjugated goat anti-rabbit and mouse IgG were purchased from ZSGB-BIO (Beijing, China).

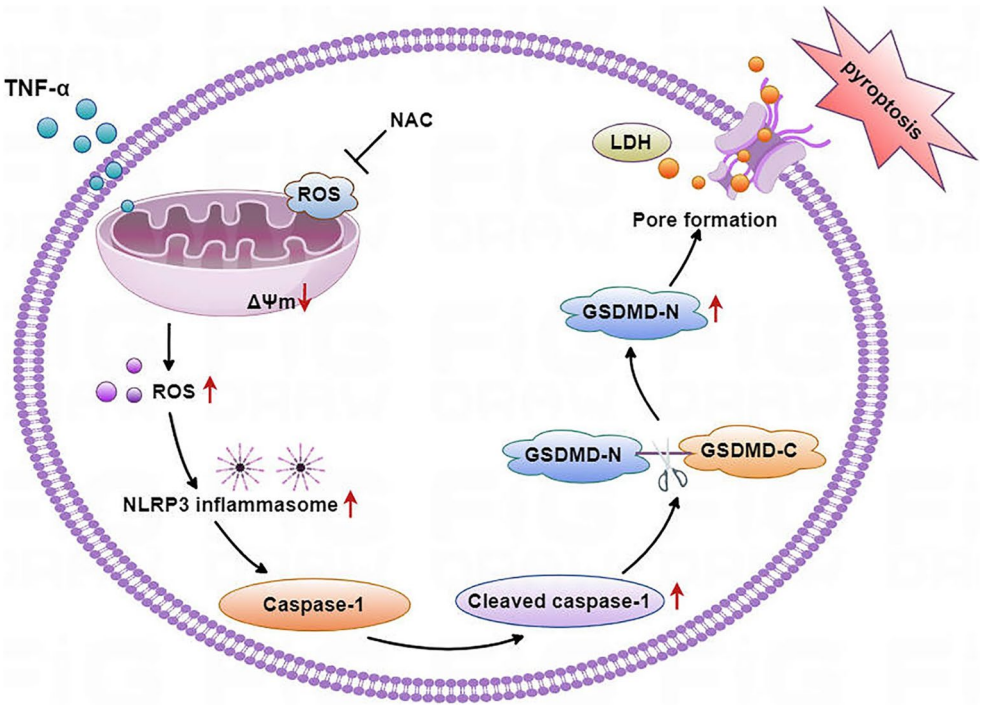

Figure 6. Potential mechanism of TNF-α-induced pyroptosis in MCF-7 cells.

Cell culture
The MCF-7 cell line was procured from Pricella Biologicals (Wuhan, China). Cells were cultured in DMEM medium containing 10% FBS and 1% Penicillin-Streptomycin solution and placed in a cell culture incubator containing 5% CO_2 at 37 °C. MCF-7 cells were subcultured every 2–3 days according to their status and density.

Cell viability assay
Logarithmic growth phase cells with good growth status were selected to make cell suspensions and then plated 5×10^3 cells per well in 96-well plates. MCF-7 cells were incubated in the incubator for 24 h and then treated with indicated concentrations of TNF-α for 48 h. Subsequently, 10 ul of CCK-8 reagent was added to each well. The plate was placed in the incubator for 2 h, and then the absorbance (OD value) was measured at a wavelength of 450 nm using a microplate reader.

Colony formation assay
Cells in the logarithmic growth phase were trypsinized and then seeded in 6-well plates at a density of 7×10^2 cells per well. The plate was incubated in an incubator at 37 °C for 24 h and continued incubating for 2 weeks after TNF-α treatment. Methanol was added to fix the cells for 10 min after PBS washing and then stained with crystal violet solution. The plate was washed several times with clean water after staying at room temperature for 5 min and then inverted in air to dry to observe the formation of clones.

Microscopy imaging
Logarithmic growth phase cells with good growth status were selected and counted for cell suspensions. MCF-7 cells were then seeded in 6-well plates with 1×10^5 cells per well. The plates were placed in the incubator and then treated with the indicated concentration of TNF-α for 48 h after cell attachment, observing the cell morphology under the microscope.

Hoechst/propidium Iodide (PI) staining
Selecting logarithmic growth phase cells in good growth condition, prepared cell suspensions, and counted. MCF-7 cells were then seeded in 12-well plates at a density of 5×10^4 per well and treated with indicated concentrations of TNF-α for 48 h after cell adhesion. 1 ml of buffer, 5 µl Hoechst, and 5 µl PI were added per well after PBS washing and incubated in the dark for 20 min, and then the cells were observed with a fluorescence microscope after PBS washing.

Lactate dehydrogenase (LDH) release assay
LDH release was considered an essential indicator of cell membrane integrity. Logarithmic growth phase cells with good growth status were selected and counted for cell suspensions. Cells were plated with 1×10^4 cells per well in 96-well plates. After the cells were adherent, they were treated with different concentrations of TNF-α, and LDH release reagents were added according to the instructions. After reaching the predetermined time, the cell culture plate was centrifuged by a multi-well plate centrifuge at 400 g for 5 min. The supernatant of each well was added to the corresponding well of a new 96-well plate, and the LDH detection working solution was added and mixed. The plate was incubated at room temperature for 30 min in the dark. The absorbance was then determined at 490 nm with a multimode microplate reader.

Elisa
ELISA kits were used to evaluate the effects of TNF-α on IL-1β and IL-18 production. MCF-7 cells were treated with different concentrations of TNF-α, and the cell supernatant was collected and centrifuged at 4 °C, 3000 rpm for 15 min. The IL-18 and IL-1β content in cell supernatant of different groups was then measured by ELISA kit according to the manufacturer's instructions.

Western blotting analysis
RIPA Lysis Buffer was added to MCF-7 cells and lysed on a shaker for 30 min. Once lysis was completed, cells were collected by centrifugation at 12,000 rpm/min for 15 min at 4 °C. The concentration of proteins was determined, and then the prepared protein was stored at -20 °C for later use. 10–12% SDS denaturing polyacrylamide gels were prepared, and electrophoresis was performed. Proteins were transferred onto a PVDF membrane and then blocked with 5% skim milk at room temperature with slow shaking on a shaker for 2 h. After washing with TBST, PVDF membranes were incubated with anti-NLRP3, Cleaved-Caspase-1, GSDMD, GSDMD-N, and β-actin primary antibodies overnight on a 4 °C refrigerator shaker, recovered primary antibodies the next day and then incubated PVDF membranes with HRP-conjugated rabbit/mouse secondary antibodies for 1 h at room temperature. Protein expression was detected by ECL chromogenic detection after TBST washing.

Immunofluorescence assay
MCF-7 cells were trypsinized and seeded in 12-well plates with 5×10^4 cells per well. TNF-α treatment was followed by fixation with 4% paraformaldehyde for 20 min, then permeabilized the cells with 1% Triton X-100 for 15 min and blocked with 5% BSA for 1 h at room temperature. Primary antibodies (1:100 dilution) prepared with BSA were added and incubated overnight at 4°C. After PBS washing, the fluorescent secondary antibody (1:200 dilution) was added and incubated for 1 h in the dark. After staining with hoechst33342 for 15 min, the cell crawling slides were removed and mounted with an autofluorescence quenching mountant and then observed with an inverted fluorescence microscope.

Mitochondrial membrane potential measurement

MCF-7 cells in the logarithmic growth phase were counted and seeded in 12-well plates at a density of 5×10^4 cells per well and then treated with different concentrations of TNF-α for 48 h after cell attachment. The JC-1 staining solution was added and incubated on the plate in a 37°C cell culture incubator for 20 min. After washing two times with JC-1 staining buffer, the cell culture medium was added to the plate and observed under a fluorescence microscope. When the mitochondrial membrane potential is high, JC-1 collects in the mitochondrial matrix to form a polymer, which can produce red fluorescence. In contrast, when the mitochondrial membrane potential is low, JC-1 cannot gather in the mitochondrial matrix, and JC-1 is a monomer and can create green fluorescence. The Image J program was used to analyze the JC-1 aggregates/monomers ratio.

Measurement of ROS

MCF-7 cells in the logarithmic growth phase were counted and seeded in 24-well plates at a density of 3×10^4 cells per well and then treated with different concentrations of TNF-α for 48 h after cell adhesion. Removing the old culture medium and washing the plate with PBS, the DCFH-DA working solution (10 mM) was added subsequently and incubated at 37 °C for 20 min. Then, the plate was washed three times with a serum-free medium and placed under an inverted fluorescence microscope for observation.

Statistical analysis

All experiments were repeated at least three times, and all data were presented as Mean ± SD. One-way ANOVA and Tukey's multiple comparisons test were used to analyze the significance of the intergroup differences. The data were statistically analyzed using GraphPad Prism and Image J software. $P < 0.05$ was considered statistically significant.

Data availability

All data utilized in this study are included in this article.

Received: 31 March 2024; Accepted: 18 October 2024
Published online: 29 October 2024

References

1. Sung, H. et al. Global Cancer statistics 2020: GLOBOCAN estimates of incidence and Mortality Worldwide for 36 cancers in 185 countries. *Cancer J. Clin.***71**, 209–249 (2021).
2. Fang, Y. et al. Pyroptosis: a new frontier in cancer. *Biomed. Pharmacother.***121**, 109595 (2020).
3. Faria, S. S., Costantini, S., de Lima, V. C. C., Andrade, V. P. D. & Magalhes, K. G. NLRP3 inflammasome-mediated cytokine production and pyroptosis cell death in breast cancer. *J. Biomed. Sci.***28**, 26 (2021).
4. Jiao, Y., Wang, L., Lu, L., Liu, J. & Zheng, B. The Role of Caspase-4 and NLRP1 in MCF7 Cell Pyroptosis Induced by hUCMSC-Secreted Factors. *Stem Cell Int.* **2020**, 1–14 (2020).
5. Pizato, N. et al. Omega-3 docosahexaenoic acid induces pyroptosis cell death in triple-negative breast cancer cells. *Sci. Rep.***8**, 1952 (2018).
6. Yan, H., Luo, B., Wu, X., Guan, F. & Yuan, J. Cisplatin induces pyroptosis via activation of MEG3/NLRP3/caspase-1/GSDMD pathway in Triple-negative breast Cancer. *Int. J. Biol. Sci.***17**, 2606–2621 (2021).
7. Yan, L., Liu, Y., Ma, X. F., Hou, D. & Wu, G. Triclabendazole induces pyroptosis by activating Caspase-3 to Cleave GSDME in breast Cancer cells. *Front. Pharmacol.***12**, 670081 (2021).
8. Hassan, M., Watari, H., Abualmaaty, A., Ohba, Y. & Sakuragi, N. Apoptosis and Molecular Targeting Therapy in Cancer.. *Biomed Res Int.***2014**, 150845 (2014).
9. Atzeni, F. & Sarzi-Puttini, P. Tumor Necrosis Factor - ScienceDirect. In *Brenner's Encyclopedia of Genetics* 2nd edn 229–231 (2013).
10. Lee, E., Ouzounova, M., Piranlioglu, R., Ma, M. T. & Korkaya, H. The pleiotropic effects of TNFα in breast cancer subtypes is regulated by TNFAIP3/A20. *Oncogene*. **38**, 1 (2018).
11. Lvarez, S., Blanco, A., Fresno, M., Muoz-Fernández, M. & Wolozin, B. TNF-alpha contributes to Caspase3 independent apoptosis in Neuroblastoma cells: role of NFAT. *PLoS ONE.* **6**, e16100(2011).
12. Shen, W. H. *Mechanisms of Cytokine-Induced IGF -I insensitivity in Cancer cells* (2003).
13. Liu, Y. et al. Anti-apoptotic effect of claudin-1 on TNF-α-induced apoptosis in human breast cancer MCF-7 cells. *Tumor Biology*. **33**, 2307–2315 (2012).
14. Li, Q. et al. Gelsolin, but not its cleavage, is required for TNF-induced ROS generation and apoptosis in MCF-7 cells. *Biochem. Biophys. Res. Commun.***385**, 284–289 (2009).
15. Galluzzi, L., Vitale, I., Aaronson, S. A., Abrams, J. M. & Kroemer, G. Molecular mechanisms of cell death: recommendations of the nomenclature Committee on Cell Death 2018. *Cell Death Differ.* **25**, 486-541 (2018).
16. Shuo et al. The mechanisms of NLRP3 inflammasome/pyroptosis activation and their role in Parkinson"s disease. *Int. Immunopharmacol.***67**, 458–464 (2018).
17. Wu, X. et al. Nicotine promotes atherosclerosis via ROS-NLRP3-mediated endothelial cell pyroptosis. *Cell Death Dis.***9**, 171 (2018).
18. Chen, X., Liu, G., Yuan, Y., Wu, G. & Yuan, L. NEK7 interacts with NLRP3 to modulate the pyroptosis in inflammatory bowel disease via NF-κB signaling. *Cell Death Dis.***10**, 906 (2019).
19. Sborgi, L. et al. GSDMD membrane pore formation constitutes the mechanism of pyroptotic cell death. *EMBO J.* **35**,1766-78 (2016).
20. Shi et al. Cleavage of GSDMD by inflammatory caspases determines pyroptotic cell death. *Nature.* **526**,660-5 (2015).
21. Shi, J., Gao, W., & Shao, F. Pyroptosis Gasdermin-mediated programmed necrotic cell death. *Trends Biochem. Sci.* **42**,245-254 (2017).
22. Liu, X., Zhang, Z., Ruan, J., Pan, Y., Magupalli, V. G., Wu, H.,& Lieberman,J. Inflammasome-activated gasdermin D causes pyroptosis by forming membrane pores. *Nature.* **535**,153-158 (2016).
23. Xia, X., Wang, X., Cheng, Z., Qin, W. & Hu, J. The role of pyroptosis in cancer: pro-cancer or pro-host? *Cell Death Dis.***10**,650 (2019).
24. Xixi, Zhang, H. & Zhang,. Chemotherapy drugs induce pyroptosis through caspase-3-dependent cleavage of GSDME. *Sci. China(Life Sciences)***v.61**, 129–130 (2018).
25. Fuchs, Y. & Steller, H. Programmed cell death in animal development and disease. *Cell.* **147**, 742–758 (2011).

26. Barcenas, C. H. Annual Report to the Nation on the Status of Cancer, 1975–2011, Featuring Incidence of Breast Cancer Subtypes by Race/Ethnicity, Poverty, and State. In *(North American Association of Central Cancer Registries, Springf. Breast Diseases: A Year Book Quarterly* Vol. 27 (eds BA, Kohler, Sherman, R. L., Howlader, N. et al.) 36–38 (2016).
27. Nicolini, A., Carpi, A. & Rossi, G. Cytokines in breast Cancer. *Cytokine & Growth Factor Reviews*. **17**,325-337 (2006).
28. Ooppachai, C., Dejkriengkraikul, P. L. & Yodkeeree, S. Dicentrine potentiates TNF-α-Induced apoptosis and suppresses Invasion of A549 lung adenocarcinoma cells via modulation of NF-κB and AP-1 activation. *Molecules*. **24**, 4100 (2019).
29. Manda, T. et al. The efficacy of combined treatment with recombinant human tumor necrosis factor-α and 5-fluorouracil is dependent on the development of capillaries in tumor. *Eur. J. Cancer*. **26**, 93–99 (1990).
30. Changli, J. et al. Tumor vasculature-targeted recombinant Mutated Human TNF-α enhanced the anti-tumor activity of Doxorubicin by increasing Tumor Vessel permeability in mouse xenograft models. *Plos One*. **9**, e87036 (2014).
31. Jiang, Y. et al. STAT1 mediates transmembrane TNF-alpha-induced formation of death-inducing signaling complex and apoptotic signaling via TNFR1. *Cell. Death Differ.***24**, 660–671 (2017).
32. Aggarwal, R. B. B. TNF-Induced Signaling in apoptosis. *J. Clin. Immunol.***19**,350-64 (1999).
33. Wang, Y., Zhang, H., Chen, Q., Jiao, F. & Gong, Z. TNF-α/HMGB1 inflammation signaling pathway regulates pyroptosis during liver failure and acute kidney injury. *Cell Prolif.* **53**, e12829 (2020).
34. Zhai, Z., Yang, F., Xu, W., Han, J., Luo,G. & Sun, E. Attenuation of Rheumatoid Arthritis Through the Inhibition of Tumor Necrosis Factor–Induced Caspase 3/Gasdermin E–Mediated Pyroptosis. *Arthritis & Rheumatology.* **74**, 427-440 (2022).
35. Jiwei et al. TNF-α-induced NF-κB activation promotes myofibroblast differentiation of LR-MSCs and exacerbates bleomycin-induced pulmonary fibrosis. *J. Cell. Physiol.* **233**,2409-2419 (2018).
36. Hou, J. et al. PD-L1-mediated gasdermin C expression switches apoptosis to pyroptosis in cancer cells and facilitates tumor necrosis. *Nat. Cell Biol.* **22**,1264-1275 (2020).
37. Hu, L., Chen, M., Chen, X., Zhao, C. & Dai, H. Chemotherapy-induced pyroptosis is mediated by BAK/BAX-caspase-3-GSDME pathway and inhibited by 2-bromopalmitate. *Cell Death Dis.* **11**, 281 (2020).
38. Montero, J., Dutta, C., Van Bodegom, D., Weinstock, D. & Letai, A. p53 regulates a non-apoptotic death induced by ROS. *Cell. Death Differ.***20**, 1465–1474 (2013).
39. Wang, Y. et al. Mitochondrial ROS promote macrophage pyroptosis by inducing GSDMD oxidation. *J. Mol. Cell. Biol.***11**, 1069–1082 (2019).
40. Yang, X., Chen, G., Yu, K. N., Yang, M. & Han, W. Cold atmospheric plasma induces GSDME-dependent pyroptotic signaling pathway via ROS generation in tumor cells. *Cell Death Dis.* **11**, 295 (2020).
41. Zhang, Z. et al. Caspase-3-mediated GSDME induced pyroptosis in breast cancer cells through the ROS/JNK signaling pathway. *J. Cell. Mol. Med.* **25**, 8159-8168 (2021).
42. Aggarwal, V. et al. Role of Reactive Oxygen Species in Cancer Progression: Molecular Mechanisms and Recent Advancements. *Biomolecules*. **9**, 735 (2019).
43. Li, Y. et al. Lobaplatin induces BGC-823 human gastric carcinoma cell apoptosis via ROS- mitochondrial apoptotic pathway and impairs cell migration and invasion. *Biomed. Pharmacother.***83**, 1239–1246 (2016).
44. Xie, W. et al. Simvastatin induces pyroptosis via ROS/caspase-1/GSDMD pathway in colon cancer. *Cell. Communication Signal.* **21**, 329 (2023).
45. Yang, Y., Liu, P. Y., Bao, W., Chen, S. J. & Zhu, P. Y. Hydrogen inhibits endometrial cancer growth via a ROS/NLRP3/caspase-1/GSDMD-mediated pyroptotic pathway. *BMC Cancer.* **20**, 28 (2020).
46. An, H. et al. Tetraarsenic hexoxide enhances generation of mitochondrial ROS to promote pyroptosis by inducing the activation of caspase-3/GSDME in triple-negative breast cancer cells. *Cell. Death Dis.***12**, 159 (2021).

Acknowledgements

We would like to thank all those involved in the experiment for their contributions to this study and the experimental environment provided by the laboratory.

Author contributions

K.G. and P.S. designed the research; K.G.,Y.L. and C.S. performed the majority of research; G.L. organized the data. Y.W. and J.O. analyzed the data; K.G. and H.B. drafted the manuscript. P.S. supervised the entire study and reviewed the manuscript.All authors read and approved the final manuscript.

Funding

This study was supported by grants from the Basic Scientific Research and Business Expenses Project of Heilongjiang Province (2022-KYYWF-0704), the Medical and Health Scientific Research Project of Heilongjiang Province (20220101020737), the Heilongjiang Natural Science Foundation (JQ2021H004).

Declarations

Consent for publication

All authors agree to publish this article.

Competing interests

The authors declare no competing interests.

Additional information

Supplementary Information The online version contains supplementary material available at https://doi.org/10.1038/s41598-024-76997-4.

Correspondence and requests for materials should be addressed to P.S.